Journal of Spectroscopy and Molecular Sciences

Journal Homepage: https://dergipark.org.tr/tr/pub/jsms

Ab-initio study aiming some spectroscopic and electronic properties of 2-[(1H-benzimidazol-1-yl)- methyl]benzoic acid

Eylem Çelik[1,2,*], Pınar Tunay Taşlı[1], Sevgi Ozdemir Kart[1,*]

[1]Pamukkale University, Art & Science Faculty, Department of Physics, Denizli, Türkiye

[2]Pamukkale University, Faculty of Sport Sciences, Department of Coaching Education, Denizli, Türkiye

*Correspondence: eylemc@pau.edu.tr (Eylem Çelik), ozsev@pau.edu.tr (Sevgi Ozdemir Kart)

ORCIDs Eylem Çelik: https://orcid.org/0000-0002-3941-1793
Pınar Tunay Taşlı: https://orcid.org/0000-0001-6580-9765
Sevgi Ozdemir Kart: https://orcid.org/0000-0001-5706-7722

Abstract: In this study, our main aim to characterize the title molecule of $C_{15}H_{12}N_2O_2$ by using quantum chemistry computational method. We have performed ab-initio simulations to determine the quantized energy levels of molecules, ions or nuclei, which enable to obtain its structural parameters and, some spectroscopic, electronic and thermal properties. The compound is optimized by using ab-initio method based on the density functional theory (DFT)/B3LYP with 6-31G(d,p) basis set implemented in Gaussian 09W subprogram. The geometric parameters of bond length, bond angle and dihedral angle computed are in good agreement with those of available experiment. The same basis set and computational method have been utilized for the vibrational spectra of the title compound by using the optimized structure. The marking of the vibrational wavenumbers of the molecule have been carried out via the VEDA4 program (Vibrational Energy Distribution Analysis). The title molecule has 31 atoms and 87 fundamental vibrational modes, with the most bending vibrations. Since experimental chemical shifts are generally obtained in DMSO (Dimethyl Sulfoxide) and Acetonitrile solutions, the ^{1}H and ^{13}C NMR chemical shifts of the molecule in the same solutions are computed by using the Gauge-Independent Atomic Orbital (GIAO) approach applying DFT/B3LYP method with the basis set of 6-31G (d,p). Moreover, UV-Vis spectral analysis of the studied molecule have been investigated in both of the DMSO and Acetonitrile solvents. The maximum absorption peaks of compound have been evaluated by the Time Dependent Self-Consistent Field (TD-SCF)/DFT/B3LYP/6-31G(d,p) method. A single absorbance without any shoulder at 257 nm in both solvent have been observed. At last, electronic properties such as chemical hardness/softness, ionization potential, highest occupied molecular orbital (HOMO)-lowest unoccupied molecular orbital (LUMO) energy levels, electronegativity and energy bandgap have been predicted. Thermal properties such as zero point, Gibbs free and total thermal energies of the title molecule have been evaluated. Our results from DFT calculations not only aid in the interpretation of available experimental data, but also illuminate the spectroscopic and electronic properties of the title molecule in detail.

Keywords: Benzoic acid; DFT; Vibrational spectroscopy; UV-Vis and NMR spectral analyzes.

1. Introduction

Heterocyclic compound, class of organic chemical compounds with one or more rings in which one or more carbon atoms in the ring are replaced by atoms of other elements, such as,

Received 15 June 2022, Accepted 21 December 2022, Available online 25 December 2022.
This work has been presented in TURCMOS2022.

primarily oxygen, nitrogen, and sulfur. These different atoms in the ring are called heteroatoms. Heterocyclic chemistry is the branch of organic chemistry dealing with the synthesis, properties, and applications of these heterocycles. It is notified in the studies of heterocyclic compounds that there is a wide range of their pharmacological properties occurring naturally as well as synthetically. The number of these studies has been increasing rapidly in recent years. Heterocyclic compounds essential for life are vitamins, antibiotics, hormones, alkaloids, synthetic drugs and dyes. Therefore, the knowledge of heterocyclic chemistry is useful for biosynthesis, drug metabolism, heredity, and evolution (Bansal, 2007). One of the important heterocyclic compounds is Benzimidazole.

Benzimidazoles are condensed heterocyclic molecules formed by the fusion of benzene and imidazole rings. The benzimidazole molecule has three isomers depending on the surface on which the imidazole ring is condensed. In recent years, benzimidazole and its derivatives have been widely used in the field of therapeutic agents (Palosi et al., 1990), drugs and pharmaceuticals (Valdez et al., 2002). Especially, they are found in the structure of many drugs which have a therapeutic effect in many cases, such as antifungal, antimicrobial, anti-inflammatory, anticancer, antiviral, antidiabetic, etc. In addition, it is stated that benzimidazole derivatives exhibit antitumor activity against several tumor cells such as lung cancer, and benzimidazole ring system is present in antitumor active agents (Boiani and Gonzales, 2005; Kumar et al., 2002; Aboraia et al., 2006).

Benzimidazole and its derivatives have been of interest to many studies. The crystal and molecular structure of benzimidazole has been investigated by Özbey et al. (1998). Sundaraganesan et al. (2007) have calculated the vibrational spectroscopy of benzimidazole by using Hartree Fock (HF) and Density Functional Theory (DFT) methods and compared with the corresponding experimental data which they have evaluated. The molecular structure, vibrational modes and HOMO-LUMO analysis of the 2-amino benzimidazole molecule have been performed by Sudha et al. (2010). Recently, DFT computations of physical properties for 2-Bromo-1H-Benzimidazole molecule have been carried out by Saş et al. (2014).

In this study, we are interested in 2-[(1H-benzimidazol-1-yl)-methyl]benzoic acid ($C_{15}H_{12}N_2O_2$) which has been synthesized by Ali et al. (2021). More recently, Khanum et al. (2022) have carried out DFT based simulations to characterize the title molecule as well as analysed some spectroscopic properties experimentally. In this study, we have aimed to perform detailed quantum chemical calculations to clarify the structural, spectroscopic, electronic and thermal properties of the title molecule, and compare our results with those of other studies (Arif et al., 2021; Khanum et al., 2022). The compound is optimized by using ab-initio method based on DFT/B3LYP with 6-31G(d,p) basis set implemented in Gaussian 09W (Frisch et al., 2009) subprogram (Dennington, Keith and Millam, 2009). Computations of FT-IR, ^{1}H and ^{12}C NMR, and UV-Vis spectrum are evaluated to get vibrational modes, chemical shifts, and the wavelengths at the absorption peaks of the title molecule, respectively. HOMO-LUMO energy levels are predicted to attain the electronic properties of the molecule. To our knowledge, Gibbs free, zero point and total thermal energies of the title molecule have been predicted for the first time in this study.

2. Materials and computational method

The structure of the title molecule (2-[(1H-benzimidazol-1-yl)-methyl]benzoic acid), which has been synthesized by Ali et al. (2021), are optimized by using ab-initio method based on DFT (Hohenberg and Kohn, 1964) with B3LYP hybrid function (Becke, 1993) and 6-31G(d,p) basis set implemented in Gaussian 09W program (Frisch et al., 2009). The optimized structure of the title

molecule visualized by GaussView 5.0.8 and the schematic view of the title molecule synthesized are shown in the Figure1 (a) and (b), respectively.

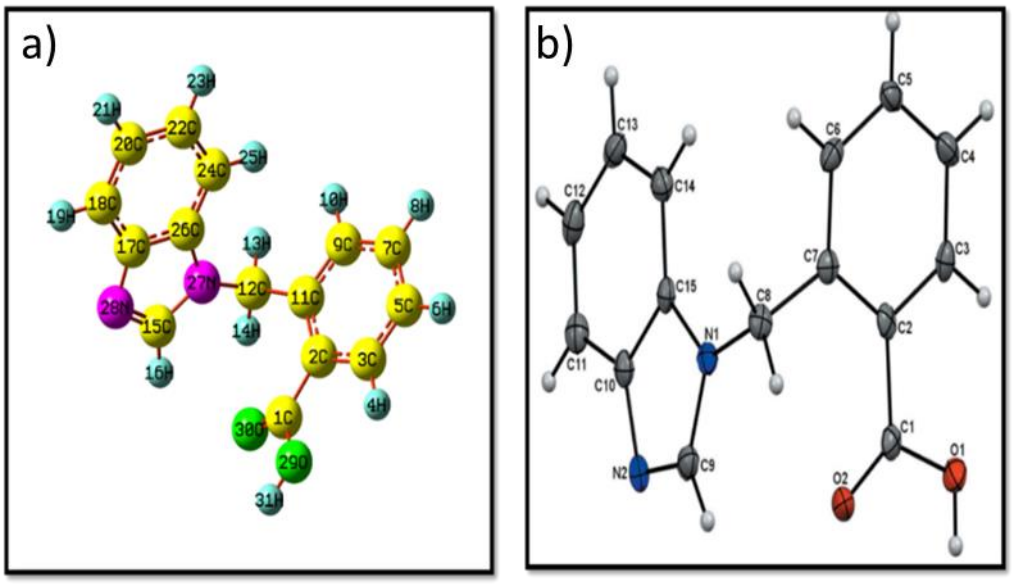

Figure 1. (a) The optimized stucture of the title molecule visualized by GaussView 5.0.8 and (b) the schematic view of the molecule synthesized by Ali et al. (2021).

The vibrational wavenumbers (FT-IR spectra) are obtained by performing DFT simulations of the optimized structure with B3LYP/6-31G (d,p). Analysis of Potential Energy Distribution (PED) are considered to make assignment of the type of vibrational mode via VEDA4 (Vibrational Energy Distribution Analysis) (Jamroz, 2004). Since the DFT computations overestimate the vibrational mode, these wavenumbers are multiplied by the scaling factor of 0.961 (Johnson, 2013) in order to adapt the calculated vibrational wavenumbers to the corresponding experimental values. The ^{1}H and ^{13}C NMR isotropic chemical shifts are predicted in DMSO and acetonitrile in solutions with the B3LYP/6-31G(d,p) basis set level by using the Gauge-Independent Atomic Orbital (GIAO) method (Ditchfield, 1972; Wolinski, Hinton, Pulay 1990). Time Dependent Self-Consistent Field (TD-SCF)/DFT/B3LYP/6-31G(d,p) based simulations are carried out to get UV-Vis spectra enable to identify the maximum absorption peaks. In order to examine the electronic structure of molecules, HOMO-LUMO (Highest Occupied Molecular Orbital-Lowest Unoccupied Molecular Orbital) energy levels of the title molecule in the ground state are computed by DFT/B3LYP/6-31G(d,p). The bandgap energy (E_g), ionization potential energy (I), electron affinity (A), electronegativity (χ), chemical hardness (η), chemical softness (s) and global electrophilicity index (ω) parameters are predicted by using Koopman's theorem which constructs the relation between HOMO-LUMO energies and these electronic properties (Sastri and Perumareddi, 1997).

3. Results and discussion

3.1. Optimized structure

The optimized structure of the title molecule given in the Figure 1(a) has total 31 atoms (15 Carbon, 12 Hydrogen, 2 Nitrogen and 2 Oxygen) and 87 fundamental vibrational modes. The structural parameters of the title molecule, such as bond length, bond angle, and dihedral angle are listed Table 1, Table 2 and Table 3, respectively. It consists of 33 bond length, 53 bond angles and 78 dihedral angles.

Table 1. The bond length (Å) of the title molecule in the ground state optimized by DFT/B3LYP 6-31G (d.p) and the corresponding experimental data (Ali et al., 2021).

	Bond Length (Å)			Bond Length (Å)	
Atoms	**Exp**	**DFT/B3LYP/ 6-31G(d,p)**	**Atoms**	**Exp**	**DFT/B3LYP/ 6-31G(d,p)**
C1-C2	1.49	1.49	C15-H16	0.95	1.08
C1-O29	1.32	1.35	C15-N27	1.36	1.38
C1-O30	1.22	1.22	C15-N28	1.31	1.31
C2-C3	1.40	1.40	C17-C18	1.39	1.40
C2-C11	1.41	1.41	C17-C26	1.41	1.42
C3-H4	0.95	1.08	C17-N28	1.39	1.40
C3-C5	1.39	1.39	C18-H19	0.95	1.09
C5-H6	0.95	1.09	C18-C20	1.39	1.39
C5-C7	1.37	1.39	C20-H21	0.95	1.09
C7-H8	0.95	1.09	C20-C22	1.40	1.41
C7-C9	1.39	1.40	C22-H23	0.95	1.09
C9-H10	0.95	1.09	C22-C24	1.38	1.39
C9-C11	1.39	1.40	C24-H25	0.95	1.08
	Bond Length (Å)			**Bond Length (Å)**	
Atoms	**Exp**	**DFT/B3LYP/ 6-31G(d,p)**	**Atoms**	**Exp**	**DFT/B3LYP/ 6-31G(d,p)**
C11-C12	1.51	1.52	C24-C26	1.39	1.40
C12-H13	1.00	1.10	C26-N27	1.39	1.39
C12-H14	0.99	1.09	O29-H31	0.88	0.97
C12-N27	1.47	1.46			

Table 2. The bond angles (°) of the title molecule in the ground state optimized by DFT/B3LYP 6-31G (d.p) and the corresponding experimental data (Ali et al., 2021).

	Bond Angles (°)			Bond Angles (°)	
Atoms	**Exp**	**DFT/B3LYP/ 6-31G(d,p)**	**Atoms**	**Exp**	**DFT/B3LYP/ 6-31G(d,p)**
C2-C1-O29	112.83	112.30	N27-C15-N28	114.31	113.60
C2-C1-O30	125.95	124.20	C18-C17-C26	120.00	121.10
O29-C1-O30	121.20	123.50	C18-C17-N28	129.55	129.70
C1-C2-C3	118.43	117.70	C26-C17-N28	110.45	109.20
C1-C2-C11	121.69	123.30	C17-C18-H19	120.04	121.25
C3-C2-C11	119.80	118.90	C17-C18-C20	118.15	117.50
C2-C3-H4	118.85	119.23	H19-C18-C20	121.81	121.25
C2-C3-C5	121.05	121.50	C18-C20-H21	119.64	119.48
H4-C3-C5	120.10	119.23	C18-C20-C22	121.22	121.00
C3-C5-H6	119.98	120.26	H21-C20-C22	119.14	119.48
C3-C5-C7	119.46	119.50	C20-C22-H23	119.28	118.94
H6-C5-C7	120.57	120.26	C20-C22-C24	121.60	122.10
C5-C7-H8	120.41	120.16	H23-C22-C24	119.12	118.94
C5-C7-C9	119.75	119.70	C22-C24-H25	120.91	121.59
H8-C7-C9	119.84	120.16	C22-C24-C26	116.95	116.80

C7-C9-H10	119.36	119.13	H25-C24-C26	122.14	121.59
C7-C9-C11	121.89	121.70	C17-C26-C24	122.08	121.50
H10-C9-C11	118.75	119.13	C17-C26-N27	104.90	105.30
C2-C11-C9	118.03	118.60	C24-C26-N27	133.02	133.20
C2-C11-C12	123.87	124.10	C12-N27-C15	126.39	125.70
C9-C11-C12	118.10	117.30	C12-N27-C26	127.58	127.90
C11-C12-H13	108.44	108.91	C15-N27-C26	105.84	106.40
C11-C12-H14	110.36	108.91	C15-N28-C17	104.51	105.40
C11-C12-N27	114.29	113.31	C1-O29-H31	105.76	111.00
H13-C12-H14	108.28	107.70			

Bond Angles (°)			Bond Angles (°)		
Atoms	**Exp**	**DFT/B3LYP/ 6-31G(d,p)**	**Atoms**	**Exp**	**DFT/B3LYP/ 6-31G(d,p)**
H13-C12-H14	108.28	107.70			
H13-C12-N27	108.34	108.91			
H14-C12-N27	107.01	108.91			
H16-C15-N27	120.10	123.20			
H16-C15-N28	125.58	123.20			

Table 3. The dihedral angles (°) of the title molecule in the ground state optimized by DFT/B3LYP 6-31G (d.p) and the corresponding experimental data.

Dihedral Angles (°)			Dihedral Angles (°)		
Atoms	**Exp**	**DFT/B3LYP/ 6-31G(d,p)**	**Atoms**	**Exp**	**DFT/B3LYP/ 6-31G(d,p)**
C1-C2-C3-C5	176.50	175.35	N28-C15-N27-C12	-179.60	-175.90
C1-C2-C11-C9	-174.80	-174.76	C18-C17-N28-C15	181.80	179.35
C1-C2-C11-C12	4.30	5.97	C17-C18-C20-C22	0.60	-0.01
C2-C3-C5-C7	-1.20	-0.07	C18-C20-C22-C24	-0.30	-0.17
C3-C5-C7-C9	1.80	0.91	C20-C22-C24-C26	-0.40	0.04
C5-C7-C9-C11	-0.20	-0.38	C22-C24-C26-C17	0.70	0.26
C7-C9-C11-C2	-1.90	-0.97	C22-C24-C26-N27	181.90	179.34
C7-C9-C11-C12	178.90	178.35	N28-C15-N27-C12	179.70	175.76
C2-C11-C12-N27	75.20	70.70	C17-C26-N27-C15	1.00	0.48
C9-C11-C12-N27	-105.60	-108.58	C24-C26-N27-C12	-1.30	-3.44
C11-C12-N27-C15	-116.80	-115.62	C24-C26-N27-C15	-180.10	-178.72
C11-C12-N27-C26	64.70	70.03			

Regression analysis of the structural parameters are conducted to compare our results with the corresponding experimental values. The results are depicted in the Figure 2. The linear regression constants for the bond length, bond angle and dihedral angle are calculated as 0.98865, 0.96461 and 0.99983 respectively, which represents that there is a good agreement between the theoretical and experimental structural parameters. These correlation values are almost close to 1 which indicates that the theoretical FT-IR spectrum calculations are successful. Therefore, it can be reported that the DFT method estimates the structural parameters quite well.

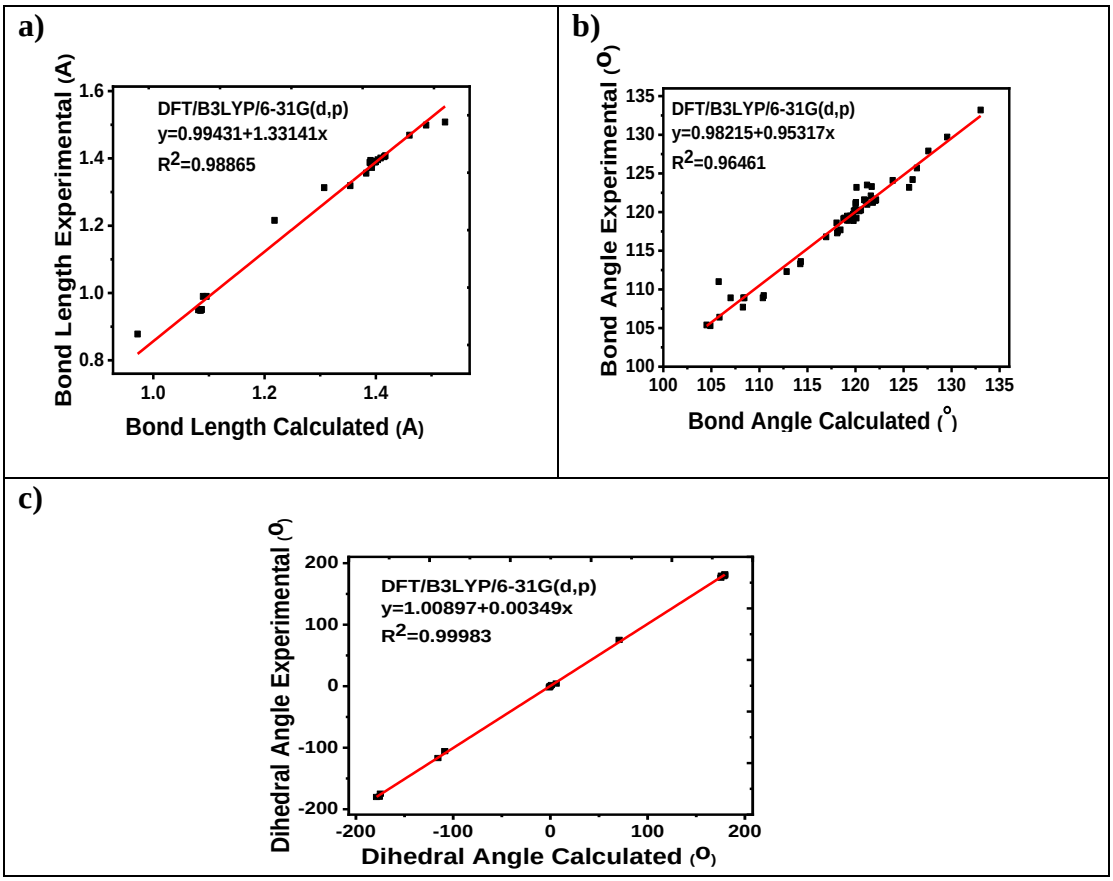

Figure 2. Linear regression of the title molecule for (a) the bond length, (b) the bond angle and (c) the dihedral angle.

3.2. FT-IR spectrum and vibrational model

The FT-IR spectrum produces valuable information about the behavior of molecular bond, intramolecular forces acting between the atoms and intermolecular forces, which enable to reveal the vibrational wavenumbers. Apart from three translational and three rotational degrees of freedom, the number of active independent fundamental modes can be determined by 3N-6 for a non-linear molecule with N atoms. Our title molecule consists of 31 atoms; thus, it has 87 normal vibrational modes. 30 (N-1) of these modes are streching, 29 (N-2) are bending and 28 (N-3) are torsion modes. Morever, our molecule has symetrical in the C1 point group.

FT-IR spectra computed for title molecule is displayed in the Figure 3. Moreover, the vibrational wavenumbers of the optimized structure obtained by DFT simulations are listed in Table 4, along with the wavenumbers multiplied by a scaling factor of 0.961 (scaled wavenumbers) due to the overestimation of the DFT calculations. The reasons for DFT calculations to be higher than the experimental values may be the use of a finite basis set, harmonic potential energy and incomplete electron correlation, and considering the interactions in gaseous form. In order to investigate the correlation between our results of vibrational wavenumbers of the title compound and the available experimental values, the root mean-square (RMS) analysis has been evaluated. It is obtained as 10.61, which is an acceptable value for DFT calculations. It can be reported that B3LYP method and 6–31G(d,p) basis set are quite suitable for explaining the spectroscopic properties of the title molecule.

Also given in Table 4 are the IR intensities and the assignments of vibrational modes by using PED analysis. The title molecule with 87 vibrational modes exhibits stretching, bending, torsion and a few mixed vibrations as seen in Table 4.

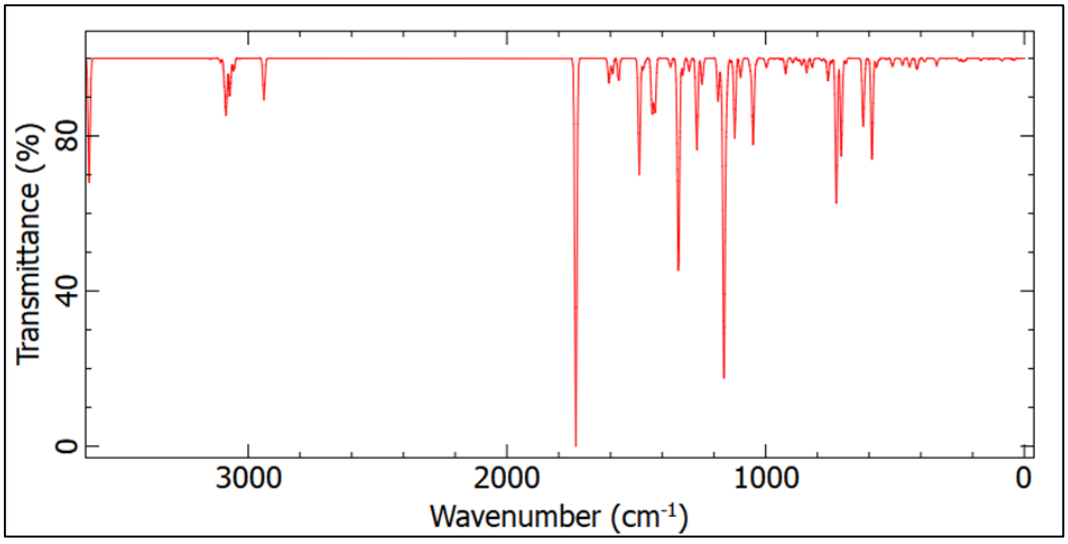

Figure 3. FT-IR spectra of the title molecule.

Heteroaromatic compounds show C–H stretching vibrations in the typical region of 3100–3000 cm^{-1} (Varsanyi et al., 1973). In this study, C–H stretching vibrations are observed at 3145 – 2939 cm^{-1}, as shown in Table 4 and Figure 3, while they are predicted as 3123-2927 cm^{-1} by other DFT study (Khanum et al., 2022), which reflects that they are in good agreement with each other. C–C aromatic stretching vibrations produce different bands covering the spectral range of 1600 to 1400 cm^{-1} (Wade, 1992). C-C stretching vibrations in the benzene ring take place in the range of 1625–1430 cm^{-1} (Jeyavijayan and Arivazhagan, 2010). As for our DFT calculations, the stretching vibrations of the C–C bond display at the values of 1037, 1295, 1591 and 1605 cm^{-1} in FT-IR spectra with PED contributions of 72%, 60%, 68% and 54%, respectively. However, Khanum et al. (2022) have evaluated that C-C bond vibrations take place at two wavenumbers of 1279 and 1588 cm^{-1} with the PED contributions of 34% and 36%, respectively.

Due to the different electronegativity of the carbon and oxygen atoms, the bond electrons are not evenly distributed between the C and O atoms (Nagabalasubramanian et al., 2012). The strongest C=O streching band peak is typically observed in the range of 1650 – 1800 cm^{-1} (Lin-Vien et al., 1991). Similarly, we have calculated this single band peak as 1733 cm^{-1} with 83% PED contribution, as seen in Figure 4. Khanum et al. (2022) have stated that the O-H bond shows a completely stretching vibration at a wave number of 3619 cm^{-1} by using DFT/B3LYP/6-311++G(d,p) for the title molecule. We have confirmed this result by predicting it as 3615 cm^{-1} by utilizing DFT/B3LYP/631G(d,p) basis set. The PED contribution of the C=O stretching vibrations 100%, which indicates that the vibration is pure stretching.

The 6-31++G(d,p) basis set used by Khanum et al (2022) is to define the diffusion functions for both hydrogen and heavy atoms. In this work, we used the 6-31G(d,p) basis set to describe the interactions between the atoms. The molecular vibration results in both studies are quite similar. It can be said that the calculation results by using the basis set with diffusion functions do not affect the vibration results much.

Table 4. The measured FT-IR (Khanum et al., 2022) and the calculated wavenumbers of the title molecule via the DFT levels with basis set of 6-31G(d,p) in the unit of cm^{-1}, IR intensities (Km. mol^{-1}) and assignments with PED (obtained from DFT/B3LYP/6-31G(d,p) percentage in the brackets. The value of 0.961 is used as a scale factor the DFT/B3LYP methods with 6-31G(d,p) basis set.

FT-IR (cm^{-1})					
DFT/B3LYP/6-31G(d,p)					Vibration modes
Mode	Unscaled	Scaled	I^{IR}	Experiment	[a]Assignment[PED] >10%
1	17	17	0.06		τCCCN(31)+τCCNC(47)
2	40	39	1.23		δCCN(16)+τCCCC(14)+τOCCC(18)+γCCCN(32)
3	51	49	0.32		τCCCN(11)+τOCCC(31)+τCCNC(10)+γCCCN(15)
4	90	87	1.64		τCCCN(15)+τOCCC(33)+τCCNC(21)
5	124	119	0.26		τCCCC(14)+τCCCN(12)+τOCCC(10)+γCCCC(11)
6	141	136	0.35		δCNC(14)+τCCCC(14)+γCCCC(14)
7	175	168	1.24		δCNC(24)+τCCCC(12)+γCCCC(17)
8	238	229	1.67		τCCCN(41)+τCNCN(13)+γCNCC(15)
9	247	237	1.77		δCCC(16)+τCCCC(10)
10	260	250	1.56		δOCC(24)+δCCC(35)
11	313	300	1.20		δCCN(12)+γCCCN(11)+γCCNC(11)
12	352	338	5.23		δCCC(32)
13	401	385	2.31		νCC(22)+δOCO(14)
14	429	412	4.61		τCCCC(19)+τCCCC(15)+γCCCC(11)
15	434	417	5.09	420	τHCCC(11)+τCCCC(14)+γCCNC(19)+γCNCC(41)
16	461	443	6.04		δOCC(13)+τCCCC(12)
17	489	470	4.83	461	δCCN(18)+δCNC(18)
18	530	509	5.73		δOCC(26)+τCCCC(11)
19	554	533	0.45		νNC(10)+δCCC(13)+δCCC(15)+δCCC(12)
20	584	561	0.88		τCCCN(30)+τCNCN(15)+τCNCN(11)
21	594	570	0.06		δCCC(11)+δCNC(10)
22	612	588	71.34		τHOCC(71)
23	626	602	0.83		τCNCN(35)
24	642	617	6.28		τCNCN(18)
25	648	622	45.50		δOCO(36)+δCCC(17)
26	718	690	3.22		τCCCC(44)
27	736	707	69.01		γOCOC(21)
28	755	725	46.15	740	τHCCN(21)+τHCCC(32)+τHCCC(33)
29	756	727	58.81		δCCC(11)
30	775	745	2.82		τCCCC(22)+τCNCN(29)+γCCNC(13)+γCNCC(19)
31	789	758	15.67		νCC(24)+δCNC(13)+δCNC(10)
32	801	769	1.44		δCNC(11)
33	814	782	1.45		γOCOC(40)+γCCCC(16)
34	852	819	5.10		νCC(18)+δCCC(20)
35	856	822	1.54		τHCCN(34)+τHCCC(38)
36	875	841	10.26		τHCNC(75)
37	895	860	4.84		δCCC(66)+δNCN(13)
38	908	873	1.73		τHCCC(81)

39	931	894	3.11		τHCCN(20)+τHCCC(28)+τHCCC(32)
40	960	923	10.43		δHCC(16)+τHCCC(28)
41	974	936	0.08		τHCCC(71)+τCCCC(11)
42	979	940	0.68		τHCCC(83)
43	1006	967	0.29		τHCCC(87)
44	1037	997	6.34		δCNC(11)+δHCC(24)+δCCC(21)+δCCN(19)
45	1079	1037	3.14		νCC(72)
46	1090	1048	60.69		νOC(28)+δCCC(36)
47	1101	1058	7.52		νNC(14)+δCCC(18)+δNCN(19)
48	1141	1096	13.31		νCC(22)+δHCC(37)
49	1164	1119	56.43	1112	νCC(16)+νOC(12)+δHCC(11)
50	1180	1134	2.25		δHCC(59)
51	1195	1148	13.73		δHCC(63)
52	1201	1154	34.58		νNC(18)+δHCC(26)
53	1208	1161	216.76		νCC(13)+δHOC(41)
54	1218	1170	16.70		νCC(25)+δHCC(18)
55	1231	1183	30.26	1174	νNC(16)+δHCN(36)
56	1295	1245	18.34	1238	δHCN(13)+δHCC(16)
57	1316	1265	61.16		νNC(22)+δHCN(13)
58	1320	1269	5.33	1308	δHCC(35)
59	1348	1295	9.02		νCC(60)
60	1373	1320	11.44		νNC(11)+νCC(12)
61	1389	1335	74.36		νCC(17)+νNC(12)+δHOC(22)+δOCO(11)
62	1392	1338	87.85		νNC(12)+τHCCC(17)
63	1399	1344	4.81		νNC(23)+δHCC(28)
64	1423	1367	6.03		νNC(15)+δHCH(18)+δHCC(13)+τHCCC(10)
65	1484	1426	27.62	1404	δHCH(40)
66	1488	1430	16.15		νCC(10)+δHCC(39)
67	1497	1438	37.37		δHCC(30)+δCNC(11)
68	1525	1466	1.69		νCC(16)+δHCC(34)
69	1533	1473	7.87		δHCC(47)
70	1548	1488	82.34		νNC(50)+δHCN(19)
71	1631	1567	13.30		νCC(35)+δCCC(20)
72	1634	1570	2.77		νCC(10)+δCCC(23)+δCNC(12)+δCCN(11)
73	1656	1591	10.55		νCC(68)
74	1670	1605	17.37		νCC(54)
75	1804	1733	274.68		νOC(83)
76	3058	2939	29.38	2919	νCH(92)
77	3155	3032	0.21		νCH(92)
78	3179	3055	6.34		νCH(95)
79	3181	3057	2.56		νCH(90)
80	3195	3070	14.74		νCH(76)
81	3196	3071	11.77		νCH(82)
82	3209	3084	13.16		νCH(91)
83	3210	3085	24.64		νCH(98)
84	3217	3092	11.43		νCH(90)

85	3234	3108	2.84		νCH(93)
86	3272	3145	0.36		νCH(99)
87	3761	3615	87.74		νOH(100)
[a]PED: potential energy distribution. ν; stretching. δ; in-plane-bending. γ; out-of plane-bending. τ; τorsion					

3.3. Absorbance spectra

The absorption spectra of the title molecule are investigated in acetonitrile and DMSO solvents by using TD-DFT/B3LYP/6-31G(d,p) method. Figure 4 presents the UV-Vis spectra of the molecule for two different solvents. The molecule absorbs the electromagnetic wave at about 257 nm in both solvents, as shown in the figure. This result shows that the title molecule may be ionized in these solvents. This absorption peak has been observed at the single point of 272 nm in DMSO solvent by the experiment performed by Khanum et al. (2022). Moreover, the same group have also computed the absorption peaks at three wavelengths of 310, 302 and 261 nm by using DFT/B3LYP/6311++G(d,p) method. This difference can be explained by the polarity of the solvent or by the strong interaction of the unbonded electrons on the oxygen in carbonyl compounds with the hydrogen of polar solvents.

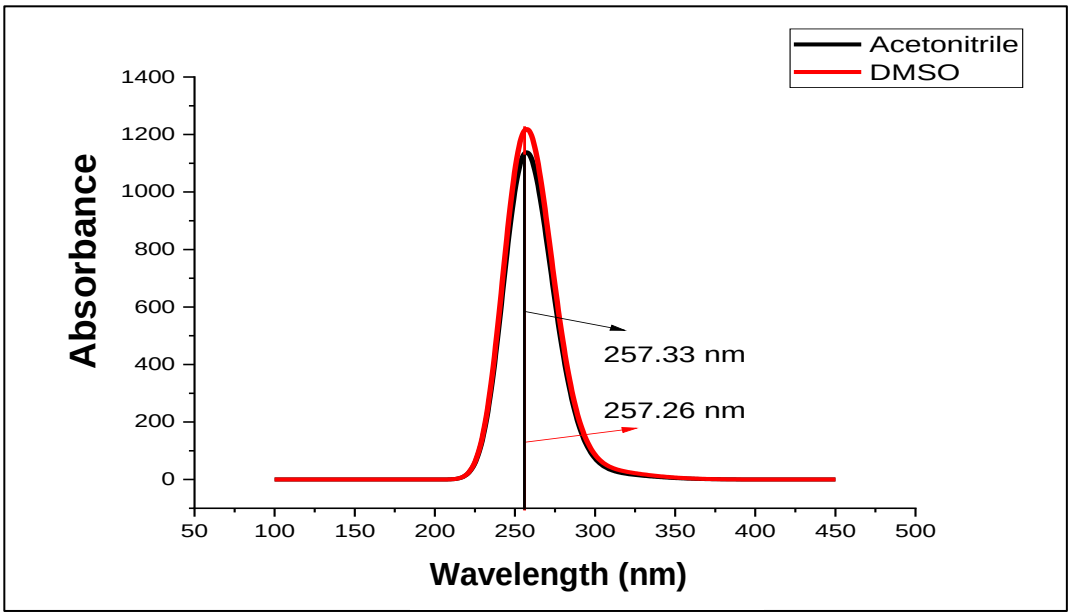

Figure 4. The calculated UV-Vis spectra of the title molecule in the solvents of DMSO and Acetonitrile.

3.4. ^{1}H and ^{12}C NMR spectra

One of the most important tools for the conformational investigation of organic molecules is ^{1}H NMR and ^{13}C NMR spectroscopy. Table 5 presents the chemical shifts from ^{1}H (proton) and ^{12}C NMR spectra computed by using DFT/B3LYP 6-31G(d,p) with GIAO approach in DMSO and acetonitrile solvents with respect to Tetramethyl-silane (TMS). Moreover, our results of proton NMR spectra in DMSO solvent are compared with those of experiment performed by Khanum et al. (2022), in the same table.

The chemical shifts of ^{1}H NMR spectra measured in DMSO solvent are presented in between 5.82 ppm to 8.25 ppm, which is verified by our results ranging between 5.11 ppm and 8.52 ppm, as

seen from Table 5. The single peak computed at 8.52 ppm is contributed from carboxylic acid protons. The chemical shifts calculated between 8.18 ppm-7.45 ppm occur due to the aromatic CH protons. This result is in good agreement with the values of the experiment ranging between 7.86 ppm-7.12 ppm (Khanum et al., 2022). Methylene protons leads to the chemical shifts occuring at 8.30 ppm, which is confirmed by the experimental value of 7.88 ppm. As for the chemical shifts of ^{13}C-NMR, they exist in between 152 ppm – 40 ppm in both DMSO and acetonitrile solvents. We could not compare our ^{13}C-NMR results with those of experiment because the ^{13}C-NMR spectrum has not been measured.

Table 5. The computed ^{1}H and ^{13}C NMR chemical shifts in the solvents of DMSO and Acetonitrile, along with the experimental value of ^{1}H NMR chemical shifts in the DMSO solvent (Khanum et al., 2022).

	Calculated Chemical Shift (ppm) via Gaussian			Calculated Chemical Shift (ppm) via Gaussian		Experimental Chemical Shift (ppm)
Carbon Atom	**DMSO**	**Acetonitrile**	**Hydrogen Atom**	**DMSO**	**Acetonitrile**	**DMSO**
1-C	152.25	152.24	**4-H**	8.53	8.53	8.25
15-C	131.04	131.03	**16-H**	8.31	8.31	7.88
17-C	129.47	129.49	**10-H**	8.19	8.18	7.86
11-C	127.31	127.32	**8-H**	8.06	8.06	7.36
26-C	120.44	120.44	**6-H**	7.84	7.84	7.32
3-C	119.55	119.56	**19-H**	7.80	7.80	7,34
7-C	119.52	119.50	**25-H**	7.79	7.80	7.15
9-C	119.10	119.08	**21-H**	7.48	7.49	7.13
5-C	114.86	114.85	**23-H**	7.45	7.45	7.12
2-C	114.32	114.33	**14-H**	6.91	6.91	6.72
22-C	108.30	108.29	**31-H**	6.54	6.54	7.14
20-C	107.04	107.03	**13-H**	5.11	5.10	5.82
18-C	105.78	105.80				
24-C	97.01	96.99				
12-C	40.73	40.74				

3.5. Electronic properties

HOMO-LUMO orbital analysis are fulfilled by the DFT/B3LYP/6-31G(d,p) method via Gaussian 09W program in order to determine the electronic and optical properties of the molecule and obtain information about its reactivation. The orbital diagram of the molecule is given in the Figure 5. Positive regions in the figure diagram are shown in red, and negative regions in green. The HOMO-LUMO energy levels of the title molecule calculated as -9.208 (eV) and -5.562 (eV), respectively.

As given in the Figure 5, the energy difference between HOMO and LUMO defined as energy bandgap of the title molecule is predicted as 3.646 eV, which represents that this molecule shows semiconductor behavior. The electronic properties such as ionization potential energy (IP), electron affinity (EA), chemical hardness (η), the electronegativity (x) and global electrophilicity index (ω) are calculated, by using HOMO-LUMO energy levels. The values of these electronic properties of the title compound are collected in the Table 6.

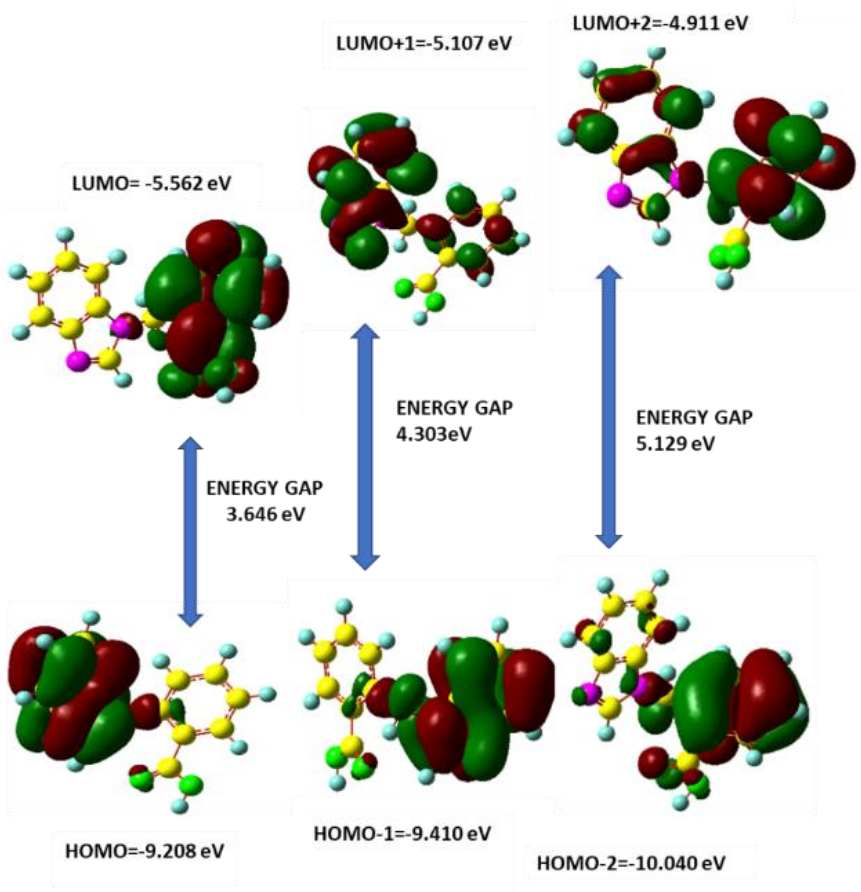

Figure 5. HOMO and LUMO energy levels of the title molecule.

The value of energy band gap indicates that this molecule presents bioactive character. The chemical hardness is calculated as 1.823 eV, which represents that the molecule is not overly rigid. The title molecule has low toxicity due to its low softness value calculated. One of the most important determinants of bioactivity is the electrophilicity index. A high value of the electrophilicity index (4.970 eV) is an indicator for examining the biological activity of the molecule, as reported by Khanum et al. (2022).

Also included in Table 6 are the results of the electronic properties predicted by Khanum et al. (2022). When we compare our results with those of their DFT study, there is good agreement with their results, except the values of HOMO-LUMO energy level, ionization potential energy and electron affinity, due to using different basis set in DFT simulations. It can be reported that the title molecule has low toxicity due to its low chemical softness value. The electrophilicity index is generally used to examine the bioactive character. The adequately high value of the electrophilicity index (4.39 and 4.97 eV), calculated by both the basis sets refers to the title molecule acting as a ligand in the biological activity and docking with a suitable protein.

Table 6. The electronic properties of the title molecule (all value in eV), along with the comparison of other DFT results by Khanum et al. (2022).

Electronic Properties (eV)	Our Result	Other Study (Khanum et al., 2022)
E_{Homo}	-9.21	−6.20
E_{Lumo}	-5.56	−2.15
Energy Band Gap (Eg)	3.65	4.05
Ionization Potential Energy (IP)	9.21	6.20
Electron Affinity (EA)	5.56	2.15
Electronegativity (x)	7.38	4.17
Chemical Hardness (η)	1.82	2.03
Chemical Softness S	0.27	0.25
Global Electrophilicity Index (ω)	4.97	4.30

3.6. Thermal properties

The enthalpy energy is important in the thermodynamics process of the molecules. The thermal correction-Gibbs free energy (ΔG) of the title molecule is optimized by using DFT/B3LYP when the sum of all kinetic and potential energies of the physical system is close to zero Joules. This provides access to thermal energy (Q). It is predicted as 161.98 kcal/mol for the molecule interested in this study. It simply indicates the energy required for the molecular system to evaporate. Zero-point energy, which shows the initial state of the system, is calculated as 152.83 kcal/mol. The enthalpy energy of the molecule is computed as approximately 162.58 kcal/mol, independent of pressure and volume, but depending on temperature. This energy refers to the amount of energy stored in the bond between atoms in a molecule. Our results for all thermal properties are collected in Table 7.

Table 7. The thermal properties of the title molecule.

Thermal properties of molecules	Hartee/Particle	kcal/mol	Joules
Zero-point energy	0.244	152.84	
Thermal correction enthalpy	0.26	162.58	
Thermal correction Gibbs free energy	0.21	125.60	0
Total thermal energy		161.99	

4. Conclusion

The structural, spectroscopic, electronical, and thermal properties of the title molecule are evaluated by DFT-based ab-initio simulations in this study. The structural properties of the molecule are comparable with those of experiment (Khanum et al., 2022), which is confirmed by linear regression constants of 0.98865, 0.96461 and 0.99983 for bond length, bond angle and dihedral angles, respectively. The percent contributions of the molecule's 87 vibrational modes and vibrational types have been determined by PED analysis. The most contribution is coming from C=O vibrations at 1733 cm^{-1}. ^{1}H and ^{13}C NMR spectra reveals the chemical shift values by the use of DFT methods. Our result of the functional group of the title molecule are in excellent good agreement with those of experiment (Khanum et al., 2022). Electronic properties related with

HOMO-LUMO interactions predicted in this study indicate that the title molecule presents bioactive character. In conclusion, it can be reported from this study that the DFT/B3LYP/6-31G(d,p) method is a very effective method for examining the structural, spectroscopic, electronic, and thermal properties of the title molecule, as well as for the identification and understanding of newly synthesized molecules. So that it can be said the title molecule could be useful for developing or enhancing the organic electronic properties of conducting materials such as metal–organic frameworks.

Acknowledgements

This study has been supported by Pamukkale University (Grant No: 2018FEBE052).

Conflict of interest

All authors state that there is no conflict of interest.

CRediT Author Statement

Author 1 (EÇ): Formal analysis, Investigation, Data Curation, Writing - Original Draft.
Author 2 (PTT): Conceptualization, Methodology, Validation.
Author 3 (SOK): Conceptualization, Methodology, Validation, Resources, Project Administration, Supervision, Writing – Review & Editing.

References

Aboraia A. S., Abdel-Rahman H. M., Mahfouz N. M., & El-Gendy M. A. 2006. Novel 5-(2-hydroxyphenyl)-3-substituted-2, 3-dihydro-1, 3, 4-oxadiazole-2-thione derivatives: Promising Anticancer Agents. Bioorganic & Medicinal Chemistry, 14(4): 1236-1246.

Ali A., Muslim M., Kamaal S., Ahmed A., Ahmad M., Shahid M., ... & Mashrai A. 2021. Crystal structure, Hirshfeld and electronic transition analysis of 2-[(1H-benzimidazol-1-yl) methyl] benzoic acid. Acta Crystallographica Section E: Crystallographic Communications, 77(7): 755-758.

Bansal R. 2007. Heterocyclic Chemistry. 4th ed. Tunbridge Wells: ANSHAN Ltd; 1-2 p.

Becke, A. D. (1993). A new mixing of Hartree–Fock and local density-functional theories. The Journal of Chemical Physics, 98(2): 1372-1377.

Boiani M., & González M. 2005. Imidazole and benzimidazole derivatives as chemotherapeutic agents. Mini Reviews in Medicinal Chemistry, 5(4): 409-424.

Dennington R., Keith T., Millam J. 2009. Semichem Inc. Shawnee Mission KS, GaussView, Version, 5.0.8

Ditchfield R. 1972. Molecular orbital theory of magnetic shielding and magnetic susceptibility. The Journal of Chemical Physics, 56(11): 5688-5691.

Frisch M., Trucks G. W., Schlegel H. B., Scuseria G. E., Robb M. A., Cheeseman J. R., ... & Fox, D. J. 2009. Gaussian 09. Gaussian Inc. Wallingford CT, 106.

Hohenberg P., Kohn W. 1964. Inhomogeneous electron gas. Physical Review, 136(3B): B864.

Jamroz, M. H. 2004. Vibrational energy distribution analysis, VEDA 4.0 Program, Warsaw.

Jeyavijayan S., Arivazhagan M. 2010. Study of density functional theory and vibrational spectra of hypoxanthine. Indian J. Pure Appl. Phys., 48: 869–874.

Johnson III, R. D. 2013. NIST computational chemistry comparison and benchmark database, NIST standard reference database number 101. Release 16a Available from: http://cccbdb. nist.gov, Retrieved 13/03/2021.

Khanum G., Ali A., Shabbir S., Fatima A., Alsaiari N., Fatima Y., Ahmad M., Siddiqui N., Javed S., Gupta M. 2022. Vibrational spectroscopy, quantum computational and molecular docking studies on 2-[(1h-benzimidazol-1-yl)-methyl] benzoic acid. Crystals, 12(3): 337.

Kumar D., Jacob, M.R., Reynolds, M.B., Kerwin, S.M. 2002. Synthesis and evaluation of anticancer benzoxazoles and benzimidazoles related to UK-1, Bioorg. Med. Chem., 10: 3997–4004.

Lin-Vien, D., Colthup, N. B., Fateley, W. G., Grasselli, J. G. 1991. The handbook of infrared and Raman characteristic frequencies of organic molecules.1st Ed. Academic Press, Boston,45-56,75 p.

Nagabalasubramanian, P. B., Karabacak, M., Periandy, S. 2012. Vibrational frequencies, structural confirmation stability and HOMO–LUMO analysis of nicotinic acid ethyl ester with experimental (FT-IR and FT-Raman) techniques and quantum mechanical calculations. Journal Of Molecular Structure, d1-13.

Özbey S., Ide S., Kendi E. 1998. The crystal and molecular structure of two benzimidazole derivatives: (phenylmethyl)-2-(4-methoxyphenylmethyl)-1H-benzimidazole-5-carboxylic acid (I) and 1,2-di-(phenylmethyl)-1H-benzimidazole-5-carboxylic acid (II)", Journal of Molecular Structure, 442: 23-30.

Palosi E. Dezso K. Erzsebet M., Szvoboda I., Laszlo H., Gyorgy S., Sandor V., Vera Katalin M. 1990. European Patent Appl. EP. 324, 988, Chem. Abstr., vol. 112, pp. 55864.

Saş, E. B., Kurt M., Can M., Okur S., İçli S., Demiç S. 2014. Structural investigation of a self-assembled monolayer material 5-[(3-methylphenyl)(phenyl) amino] isophthalic acid for organic light-emitting devices. Spectrochimica Acta Part A: Molecular and Biomolecular Spectroscopy, 133, 307-317.

Sastri V. S., Perumareddi J. R. 1997. Molecular orbital theoretical studies of some organic corrosion inhibitors. Corrosion, 53(08).

Sudha S., Karabacak M., Kurt M., Çınar M., Sundaraganesan N. 2010. Molecular structure, vibrational spectroscopic, first-order hyperpolarizability and HOMO, LUMO studies of 2-amino benzimidazole, Spectrochimica Acta Part A: Molecular and Biomolecular Spectroscopy, 84:184-195

Sundaraganesan N., Ilakiamani S., Subramani P., Joshua B. D. 2007. Comparison of experimental and ab initio HF and DFT vibrational spectra of benzimidazole. Spectrochimica Acta Part A: Molecular and Biomolecular Spectroscopy, 67(3-4): 628-635.

Wade L.G. 1992. Advanced organic chemistry, 4nd. WILEY publishing, New York, USA, 723–729. p

Wolinski K., Hinton J. F., Pulay P. 1990. Efficient implementation of the gauge-independent atomic orbital method for NMR chemical shift calculations. Journal of the American Chemical Society, 112(23): 8251-8260.

Valdez J., Cedillo R., Hernandez-Campos A., Yepez L., Hernandez-Luis F., Navarrete-Vazquez G., Tapia A., Cortes R., Hernandezc M., Castilloa R. 2002. Synthesis and antiparasitic activity of 1H-benzimidazole derivatives. Bioorg. Med. Chem. Lett., 12:2221–2224.

Varsanyi G., Kovner M. A., Láng L. 1973. Assignments for vibrational spectra of 700 benzene derivatives, AKADEMIAI KIADO. Budapest.191-212p.